

# Analytical Potential-Density Pairs for Flat Rings and Toroidal Structures

D. Vogt\*

P. S. Letelier†

Departamento de Matemática Aplicada-IMECC, Universidade  
Estadual de Campinas 13083-970 Campinas, S. P., Brazil

November 20, 2018

## Abstract

The Kuzmin-Toomre family of discs is used to construct potential-density pairs that represent flat ring structures in terms of elementary functions. Systems composed of two concentric flat rings, a central disc surrounded by one ring and a ring with a centre of attraction are also presented. The circular velocity of test particles and the epicyclic frequency of small oscillations about circular orbits are calculated for these structures. A few examples of three-dimensional potential-density pairs of “inflated” flat rings (toroidal mass distributions) are presented.

*Keywords:* planets: rings – galaxies: kinematics and dynamics.

## 1 Introduction

The presence of flat ring structures is a characteristic feature of the four giant planets of the Solar System, in particular, the famous Saturn’s rings. Planetary rings are the thinnest of all astrophysical discs, with a ratio of the thickness to the radius of order  $10^{-6}$  [1]. On a larger scale, several ring galaxies, or R galaxies, objects in the form of approximate elliptical rings with no luminous matter visible in their interiors, are known (see, for instance, [2, 3]). Sometimes, as the result of interactions between galaxies, a ring of gas and stars is formed and rotates over the poles of a galaxy, originating

---

\*e-mail: dvogt@ime.unicamp.br

†e-mail: letelier@ime.unicamp.br

the so called polar-ring galaxies ([4] and references therein). The exact gravitational potential of a ring of zero thickness and constant linear density is given by an elliptic integral, which in practice is often approximated by a truncated multipolar expansion.

The potential of a disc with negative mass density whose rim has positive mass density can be obtained by a process of complexification of the potential of a punctual mass [5, 6, 7]. This potential was used by Letelier and Oliveira [8] to construct superpositions of static bodies with axial symmetry in the context of General Relativity. An exact solution representing the superposition of a disc with a central hole and a Schwarzschild black hole was obtained by Lemos and Letelier [9]. The properties of this space-time and of space-times that represent superpositions of a Schwarzschild black-hole and a ring were investigated in [10, 11, 12].

Recently, Letelier [13] constructed several families of flat rings using the superposition of Morgan and Morgan [14] discs of different densities. The main advantage of these models is that the density and the gravitational potential are given in terms of elementary functions. The main purpose of this work is to use the same method to construct other potential-density pairs representing flat ring structures by superposing members of the classical Kuzmin-Toomre family of discs. Because the Kuzmin-Toomre discs have infinite extension, so do the resulting rings, while the Letelier rings have a finite outer radius or a central hole. All the potential-density pairs can be explicitly stated in terms of elementary functions. We construct systems composed of one and two concentric flat rings and a central Kuzmin-Toomre disc surrounded by a flat ring. By using a suitable transformation, some of these flat ring systems are used to generate three-dimensional potential-density pairs with toroidal mass distributions. Similar toroidal analytical systems have been recently obtained by Ciotti and Giampieri [15], and Ciotti and Marinacci [16] using a different technique, known as complex-shift method.

The article is divided as follows. In Section 2, we briefly revise the potential-density pair of the Kuzmin-Toomre family of discs. In Section 3, the discs are superposed to generate potential-density pairs that represent structures of one and two concentric flat rings, and a central disc surrounded by one ring. We calculate the circular velocity of particles moving inside these structures and study the stability under radial perturbations of circular orbits on the plane of the rings. We also briefly discuss the influence of a point mass located at the centre of a ring on the rotation profile and on the stability of the ring. In Section 4, we “inflate” some flat ring models by using a transformation proposed by Miyamoto and Nagai [17]. The resulting three-dimensional potential-density pairs have toroidal concentrations of matter.

In Section 5, we summarize and discuss the results. In Appendices A to F, we collect, for reference, several equations expressing potential-density pairs, circular velocities and epicyclic frequencies for the structures discussed in the main text.

## 2 Kuzmin-Toomre Discs

Kuzmin [18] derived a very simple potential-density pair of an axisymmetric disc. The potential in cylindrical coordinates  $(R, z, \varphi)$  is given by

$$\phi_0 = -\frac{GM}{\sqrt{R^2 + (a + |z|)^2}}. \quad (1)$$

By Poisson's equation, the discontinuous normal derivative on  $z = 0$  introduces a surface density of mass

$$\sigma(R) = \frac{1}{2\pi G} \left. \frac{\partial \phi}{\partial z} \right|_{z=0} = \frac{aM}{2\pi (R^2 + a^2)^{3/2}}. \quad (2)$$

The potential (1) is in fact the first member of the Kuzmin-Toomre family of discs [19]. The other members can be calculated by using the following recurrence relations [20, 21]

$$\phi_{n+1} = \phi_n - \frac{a}{2n+1} \frac{\partial}{\partial a} \phi_n, \quad (3)$$

$$\sigma_{n+1} = \sigma_n - \frac{a}{2n+1} \frac{\partial}{\partial a} \sigma_n, \quad n = 0, 1, \dots, \quad (4)$$

where  $\phi_0, \sigma_0$  is the Kuzmin potential-density pair (1)–(2). The general expression for the surface density of the  $n$ th-order Kuzmin-Toomre disc is [20]

$$\sigma_n = \frac{(2n+1)a^{2n+1}M}{2\pi(R^2 + a^2)^{n+3/2}}. \quad (5)$$

For reference the density and potential for the members with  $n = 1, 2, 3$  are listed in Appendix A.

## 3 Flat Rings

### 3.1 A Family of Single Rings

In order to generate ring structures we take Kuzmin-Toomre discs with mass

$$M = \frac{2\pi a^2 \sigma_c}{2n+1}, \quad (6)$$

where  $\sigma_c$  is a constant with dimensions of surface density. Thus the surface density (5) is rewritten as

$$\sigma_n = \frac{\sigma_c a^{2n+3}}{(R^2 + a^2)^{n+3/2}} = \frac{\sigma_c}{(1 + R^2/a^2)^{n+3/2}}. \quad (7)$$

Now let us consider the following superposition

$$\sigma^{(m,n)} = \sum_{k=0}^m C_k^m (-1)^{m-k} \sigma_{n+m-k} \quad (8)$$

$$= \frac{\sigma_c}{(1 + R^2/a^2)^{n+m+3/2}} \sum_{k=0}^m C_k^m (-1)^{m-k} \left(1 + \frac{R^2}{a^2}\right)^k, \quad (9)$$

where  $C_k^m = m! / [(m-k)!k!]$ . Using

$$\sum_{k=0}^m C_k^m (-1)^{m-k} \left(1 + \frac{R^2}{a^2}\right)^k = \left(\frac{R}{a}\right)^{2m}, \quad (10)$$

equation (8) takes the form

$$\sigma^{(m,n)} = \frac{\sigma_c (R/a)^{2m}}{(1 + R^2/a^2)^{n+m+3/2}}. \quad (11)$$

We have that (11) with  $m = 1, 2, \dots$ ;  $n = 0, 1, \dots$ , defines a family of flat rings (characterized by zero density on  $R = 0$ ) with infinite extension. For large  $R$ , the density decays as  $1/R^{2n+3}$ ; thus in principle, a cut-off radius may be defined and this flat ring is considered as finite. The density has a maximum at  $\frac{R}{a} = \left(\frac{m}{n+3/2}\right)^{1/2}$ . The total mass  $\mathcal{M}^{(m,n)}$  of member  $(m, n)$  is given by

$$\mathcal{M}^{(m,n)} = \int_{R=0}^{\infty} \int_{\varphi=0}^{2\pi} \sigma^{(m,n)} R dR d\varphi = \frac{\Gamma(m+1)\Gamma(n+1/2)}{\Gamma(m+n+3/2)} \pi \sigma_c a^2, \quad (12)$$

where  $\Gamma(x)$  is the gamma function. As  $m, n$  are integers, (12) can be further simplified to

$$\mathcal{M}^{(m,n)} = \frac{2^{m+1} m! (2n-1)!!}{(2m+2n+1)!!} \pi \sigma_c a^2. \quad (13)$$

The potentials associated with (11) can be calculated using a superposition with the same coefficients as in (8), e.g., the potential associated with

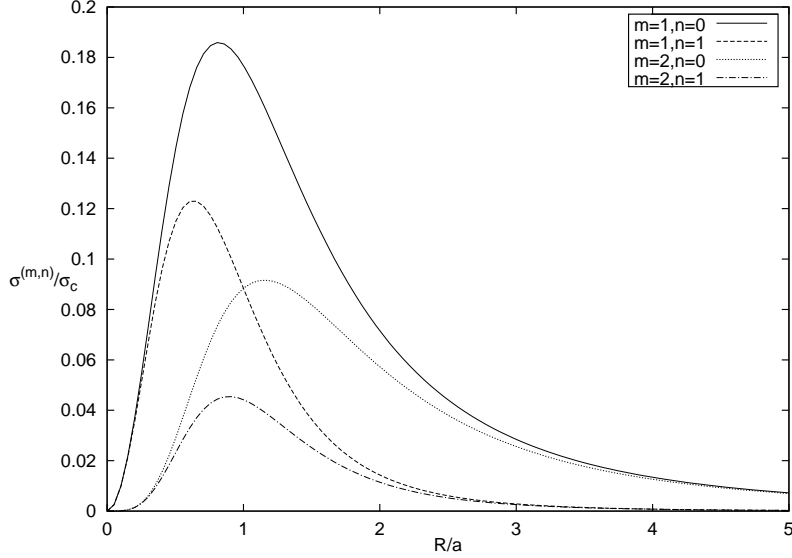


Figure 1: The surface density  $\sigma^{(m,n)}/\sigma_c$  equation (11) of four members with  $m = 1, 2; n = 0, 1$  of the family of flat single rings as function of  $R/a$ .

$\sigma^{(1,0)}$  is  $\phi^{(1,0)} = \phi_0 - \phi_1$ , etc. The explicit potential-density pairs of four members with  $m = 1, 2; n = 0, 1$  are given in Appendix B.

In Fig. 1 we show the curves of  $\sigma^{(m,n)}/\sigma_c$  as function of  $R/a$  for the four members of rings listed in equations (34)–(37). The rings with  $m = 2$  have larger central holes than those with  $m = 1$ . Also note how fast the density decays for  $n = 1$  ( $\propto R^{-5}$ ). These four members have masses  $\mathcal{M}^{(1,0)} = 4\pi\sigma_c a^2/3$ ,  $\mathcal{M}^{(1,1)} = 4\pi\sigma_c a^2/15$ ,  $\mathcal{M}^{(2,0)} = 16\pi\sigma_c a^2/15$  and  $\mathcal{M}^{(2,1)} = 16\pi\sigma_c a^2/105$ .

Some other physical quantities of interest are the circular velocity  $v_c$  of test particles concentric to the flat rings and the epicyclic frequency  $\kappa$  of small oscillations about the equilibrium circular orbit in the plane of the ring. They are calculated with the expressions [22]

$$v_c^2 = R\phi_{,R}, \quad (14)$$

$$\kappa^2 = \phi_{,RR} + \frac{3\phi_{,R}}{R}, \quad (15)$$

where the subscripts with comma indicate partial derivatives and all expressions are evaluated on  $z = 0$ . The criterion for stability is given by  $\kappa \geq 0$ . This study of stability can be considered as an order zero test of stability, where the collective behaviour of the particles of the ring is not taken into account.

Using the potential (34), we obtain the following expression for the rotation curve of the first member of the family of single rings

$$v_c^{(1,0)} = R \left[ \frac{2\pi\sigma_c G a^2 (2R^2 - a^2)}{3(R^2 + a^2)^{5/2}} \right]^{1/2}, \quad (16)$$

We have that circular orbits are only possible in the region  $R/a \geq \sqrt{2}/2 \approx 0.71$ . Near the hole of the ring, there is not enough mass to produce the necessary gravitational force to keep a particle in a circular orbit, however this can be compensated if a massive point mass is placed at the centre of the ring (see Section 3.4). The rotation curves and the expressions for the epicyclic frequency  $\kappa^{(m,n)}$  of the other members are listed in Appendix C.

In Fig. 2(a)–(b) we present, respectively, the curves of the circular velocity  $\bar{v}_c^{(m,n)} = v_c^{(m,n)}/\sqrt{\sigma_c G a}$  and of the epicyclic frequency  $\bar{\kappa}^{(m,n)} = \kappa^{(m,n)}/(\sigma_c G/a)^{1/2}$  as functions of  $R/a$  for our four members of rings. We note that the rings with  $m = 2$  have larger regions where circular orbits are not possible than rings with  $m = 1$  because the former have also larger central holes. The possible circular orbits shown are all stable under radial perturbations. In Fig. 2(b) we only plotted the curves of epicyclic frequency in the ranges where circular orbits are possible. The intervals of stability shown in equations (42)–(45) suggest that rings with larger central holes ( $m = 2$ ) also have more unstable orbits.

### 3.2 A Family of Double Rings

Now we consider the following superposition of flat rings,

$$\sigma_{(2)}^{(m,n)} = \sigma^{(m,n)} - 2k^2 \sigma^{(m+1,n-1)} + k^4 \sigma^{(m+2,n-2)} = \frac{\sigma_c (R/a)^{2m} (1 - k^2 R^2/a^2)^2}{(1 + R^2/a^2)^{n+m+3/2}}, \quad (17)$$

where  $k$  is a constant. With this superposition, a gap is placed at  $R/a = 1/k$  on a single ring, thus generating a family of two concentric flat rings. Using equation (13), the total mass of this superposition is found to be

$$\mathcal{M}_{(2)}^{(m,n)} = \frac{\pi\sigma_c a^2 2^{m+1} m!(2n-5)!!}{(2m+2n+1)!!} [(2n-1)(2n-3) - 4k^2(m+1)(2n-3) + 4k^4(m+1)(m+2)]. \quad (18)$$

We study in detail the first member of this family with  $m = 1$ ,  $n = 2$ . Its non-dimensional surface density is shown in Fig. 3 for the values  $k^2 = 2$ ,  $k^2 = 1.5$  and  $k^2 = 1$ . The size of the gap increases for smaller  $k$ .

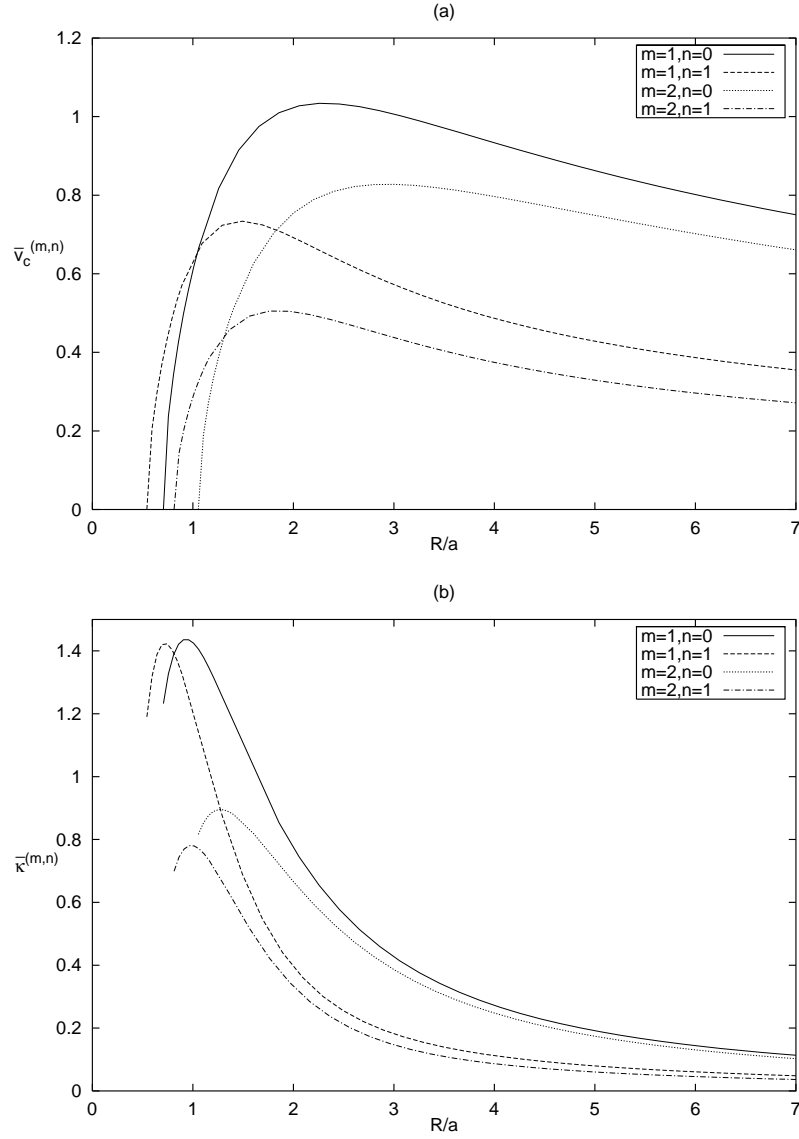


Figure 2: (a) The circular velocity  $\bar{v}_c^{(m,n)} = v_c^{(m,n)} / \sqrt{\sigma_c G a}$  equations (38)–(41) and (b) the epicyclic frequency  $\bar{\kappa}^{(m,n)} = \kappa^{(m,n)} / (\sigma_c G / a)^{1/2}$  equations (42)–(45) as functions of  $R/a$  for the four members with  $m = 1, 2$ ;  $n = 0, 1$  of the family of flat single rings.

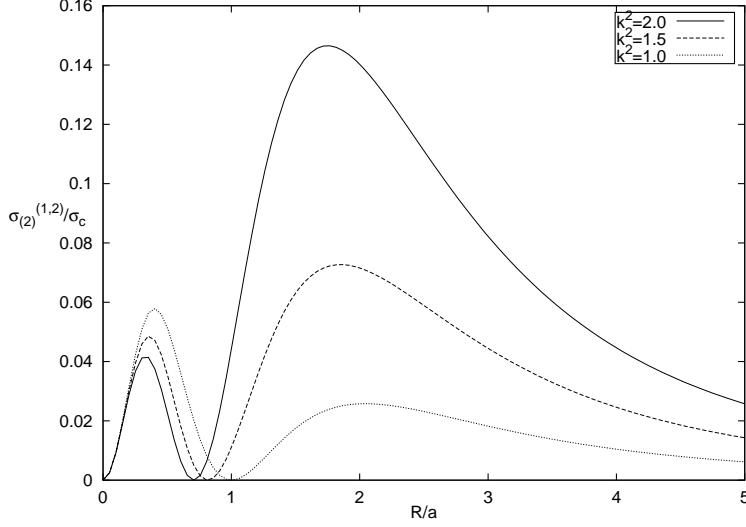


Figure 3: The surface density  $\sigma_{(2)}^{(1,2)}/\sigma_c$  of the first member of a family of double rings equation (17), as function of  $R/a$ , for  $k^2 = 2$ ,  $k^2 = 1.5$  and  $k^2 = 1$ .

The associated potential  $\phi_{(2)}^{(1,2)}$  is given by

$$\begin{aligned} \phi_{(2)}^{(1,2)} = & -\frac{2\pi\sigma_c G a^2}{105\chi^{7/2}} \left\{ 6\chi^3(1+8k^4) + \chi^2[-16k^2(R^2+|z|^2) + a^2(9-26k^2-54k^4)] \right. \\ & + 3a|z|(2-16k^2-19k^4)] - a^2\chi[2R^2(2+11k^2+9k^4) + |z|^2(1-26k^2-27k^4) \\ & \left. - a|z|(13+82k^2+69k^4) - 2a^2(7+28k^2+21k^4)] \right. \\ & \left. - 3a^3(a+|z|)(1+k^2)^2[2R^2+7(a+|z|)^2] \right\}, \quad (19) \end{aligned}$$

where  $\chi = R^2 + (a + |z|)^2$ . Expressions for the circular velocity  $v_{c(2)}^{(1,2)}$  and the epicyclic frequency  $\kappa_{(2)}^{(1,2)}$  follow from equation (19), and are listed in Appendix D.

The curves  $v_{c(2)}^{(1,2)} = 0$  (solid line) and  $\kappa_{(2)}^{(1,2)} = 0$  (dashed line) as functions of  $k$  and  $R/a$  are displayed in Fig. 4. Circular orbits are possible in the region labeled (A) delimited by the solid curve and the axes; orbits are stable in the region (B) delimited by the dashed curve and the axes. Between  $0.58 \lesssim k \lesssim 1.53$  there exist two regions where orbits are unstable and circular orbits are not possible: the first begins at the origin and the second is in



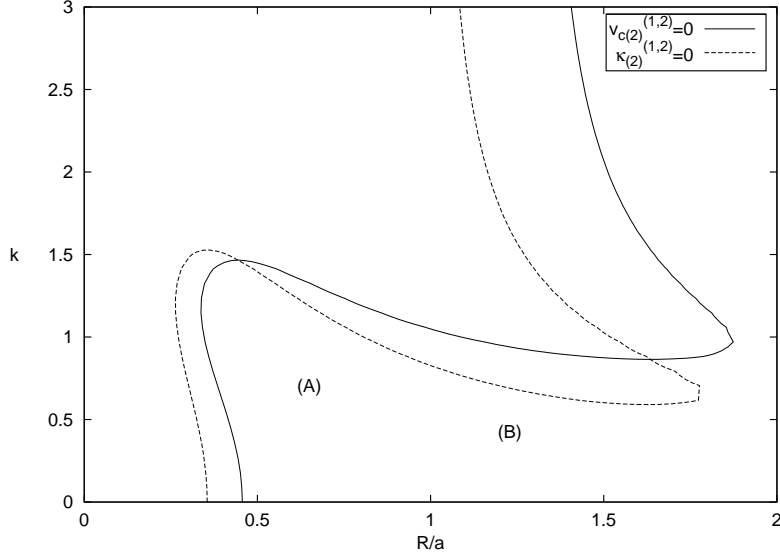


Figure 4: The curves  $v_{c(2)}^{(1,2)} = 0$  (solid line) and  $\kappa_{(2)}^{(1,2)} = 0$  (dashed line) as functions of  $k$  and  $R/a$  for the first member of a family of double rings.

an annular region. This is possibly due to the presence of the additional gap. We note that most possible circular orbits are also stable, except for the interval  $0.86 \lesssim k \lesssim 1.47$  where some parts of the double rings have unstable circular orbits. Some curves of the dimensionless circular velocity  $\bar{v}_{c(2)}^{(1,2)} = v_{c(2)}^{(1,2)} / \sqrt{\sigma_c G a}$  and dimensionless epicyclic frequency  $\bar{\kappa}_{(2)}^{(1,2)} = \kappa_{(2)}^{(1,2)} / (\sigma_c G / a)^{1/2}$  for  $k = 0.5$ ,  $k = 1$ ,  $k = 1.5$  and  $k = 2$  are depicted in Fig. 5(a) and Fig. 5(b), respectively.

### 3.3 Discs with Flat Rings

It is also possible to construct potential-density pairs for a Kuzmin-Toomre disc surrounded by a concentric flat single ring. For this, we consider the superposition

$$\sigma_{(d)}^{(n)} = \sigma_n - 2k^2 \sigma^{(1,n-1)} + k^4 \sigma^{(2,n-2)} = \frac{\sigma_c (1 - k^2 R^2 / a^2)^2}{(1 + R^2 / a^2)^{n+3/2}}. \quad (20)$$

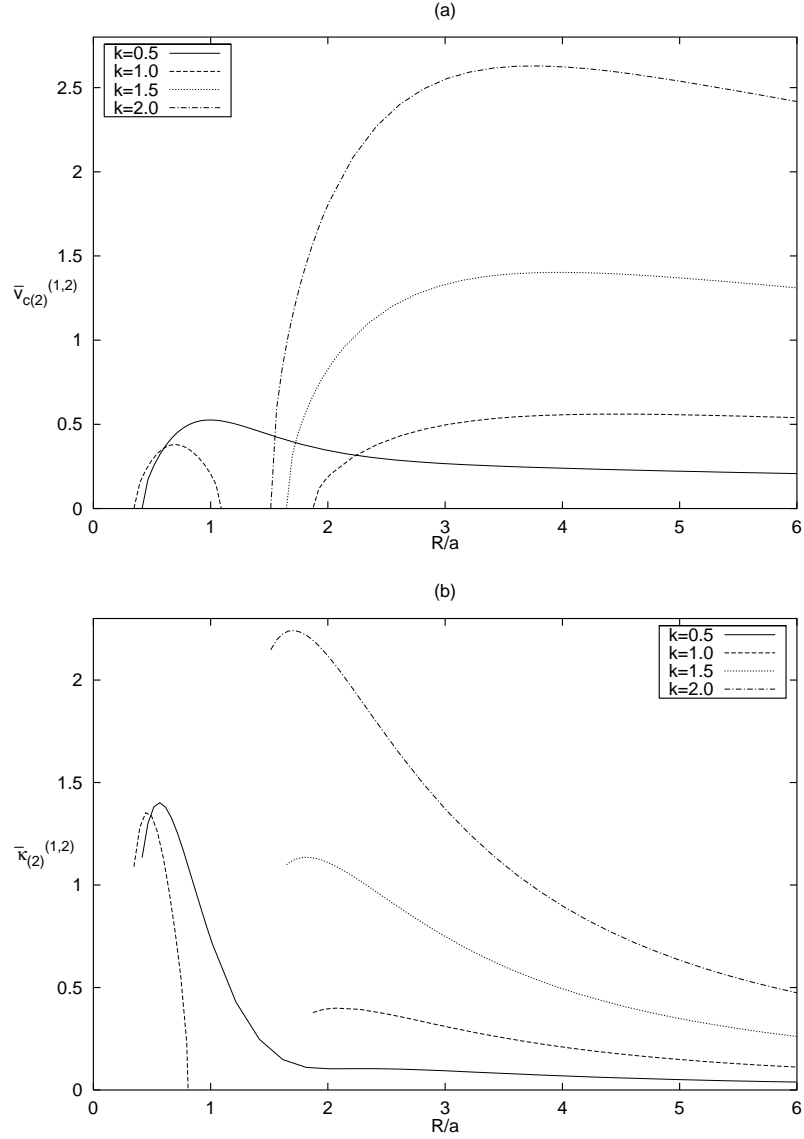


Figure 5: (a) The circular velocity  $\bar{v}_{c(2)}^{(1,2)} = v_{c(2)}^{(1,2)} / \sqrt{\sigma_c G a}$  equation (46) and (b) the epicyclic frequency  $\bar{\kappa}_{(2)}^{(1,2)} = \kappa_{(2)}^{(1,2)} / (\sigma_c G / a)^{1/2}$  equation (47) for the first member of a family of double rings as functions of  $R/a$  for  $k = 0.5$ ,  $k = 1$ ,  $k = 1.5$  and  $k = 2$ .

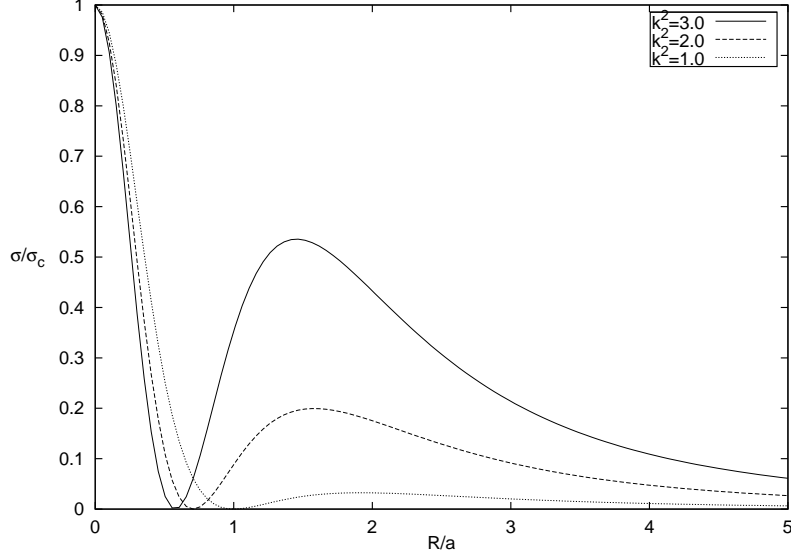


Figure 6: The surface density  $\sigma_{(d)}^{(2)}/\sigma_c$  for the first member of a family of disc and ring (20), as function of  $R/a$ , for  $k^2 = 3$ ,  $k^2 = 2$  and  $k^2 = 1$ .

Equation (20) represents the density of a disc with radius  $R/a = 1/k$  and a flat ring between  $1/k < R/a < \infty$ . The total mass of this superposition is

$$\mathcal{M}_{(d)}^{(n)} = \frac{2\pi\sigma_c a^2}{(2n+1)(2n-1)(2n-3)} [(2n-1)(2n-3) - 4k^2(2n-3) + 8k^4]. \quad (21)$$

Again we study the first member of this family with  $n = 2$ . In Fig. 6 the non-dimensional surface density  $\sigma_{(d)}^{(2)}/\sigma_c$  is shown for the values  $k^2 = 3$ ,  $k^2 = 2$  and  $k^2 = 1$ . For large values of  $k$ , the density of the ring is more concentrated. The associated potential  $\phi_{(d)}^{(2)}$  can be expressed as

$$\begin{aligned} \phi_{(d)}^{(2)} = -\frac{2\pi\sigma_c G a^2}{15\chi^{5/2}} \left\{ \chi^2(3-4k^2) + \chi[a(a+|z|)(3-4k^2) + k^4(8R^2 + 8|z|^2 + 9a|z|)] \right. \\ \left. + a^2[-R^2(1+2k^2) + (a+|z|)^2(2+4k^2+3k^4)] \right\}, \quad (22) \end{aligned}$$

where  $\chi = R^2 + (a + |z|)^2$ . By using equation (22), expressions for the circular velocity  $v_{c(d)}^{(2)}$  and the epicyclic frequency  $\kappa_{(d)}^{(2)}$  can be calculated; they are given in Appendix E.

The curves  $v_{c(d)}^{(2)} = 0$  (solid line) and  $\kappa_{(d)}^{(2)} = 0$  (dashed line) as functions of  $k$  and  $R/a$  are shown in Fig. 7. In the region (A), delimited by the solid

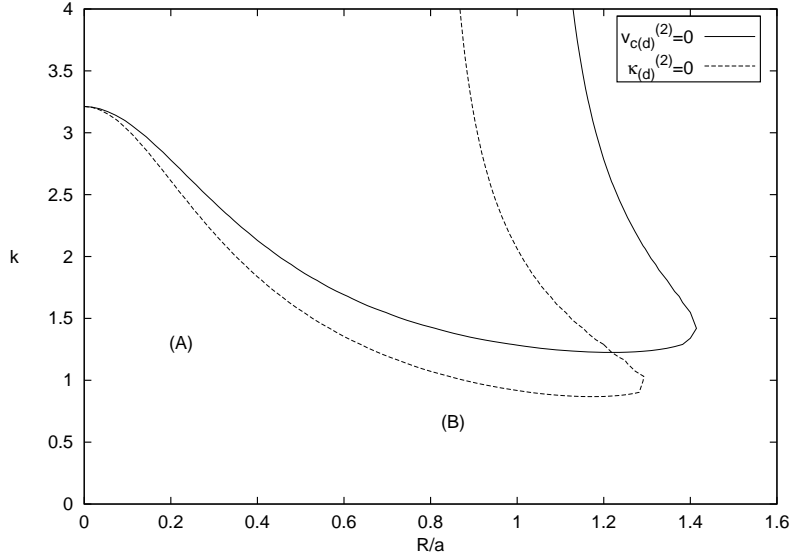


Figure 7: The curves  $v_{c(d)}^{(2)} = 0$  (solid lines) and  $\kappa_{(d)}^{(2)} = 0$  (dashed lines) as functions of  $k$  and  $R/a$  for the first member of a superposition of disc and ring.

curve and the axes, circular orbits are possible and in region (B), delimited by the dashed curve and the axes, we have stability. In the limit  $k = 0$ , we have a pure disc that is stable and all circular orbits are possible. As the value of  $k$  grows, the influence of the outer ring on the rotation curves and stability becomes more pronounced. In the interval  $0 \leq k \lesssim 0.86$ , all circular orbits are also stable. When  $1.22 \lesssim k \lesssim 3.21$ , there exist possible circular orbits that are unstable. For  $k \gtrsim 3.21$ , all possible circular orbits are stable. Curves for the circular velocity and epicyclic frequency are qualitatively similar to those for the two-ring system.

### 3.4 A Planet and a Ring

Now we study a very simple example of a planet located at the centre of a ring. Let us consider a point mass with potential  $\phi = -Gm/R$  and the first member of the family of single rings with potential  $\phi^{(1,0)}$ , equation (34). The rotation curve and epicyclic frequency of particles orbiting this planet-ring

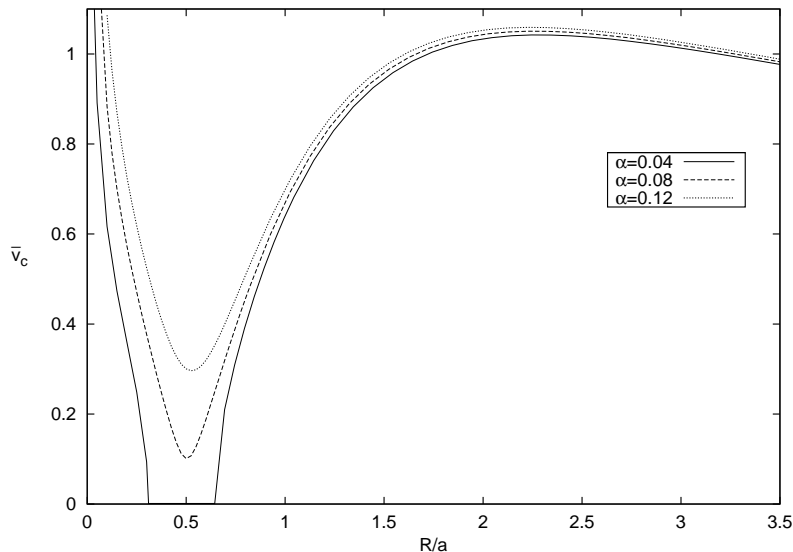


Figure 8: The circular velocity  $\bar{v}_c = v_c/\sqrt{\sigma_c G a}$  equation (23) for a planet-ring system as function of  $R/a$  for  $\alpha = m/(\sigma_c a^2) = 0.04$ ,  $\alpha = 0.08$  and  $\alpha = 0.12$ .

system are given by

$$v_c = \left[ \frac{Gm}{R} + \frac{2\pi\sigma_c G a^2 R^2 (2R^2 - a^2)}{3(R^2 + a^2)^{5/2}} \right]^{1/2}, \quad (23)$$

$$\kappa = \left[ \frac{Gm}{R^3} + \frac{2\pi\sigma_c G a^2}{3(R^2 + a^2)^{7/2}} (2R^4 + 13R^2 a^2 - 4a^4) \right]^{1/2}, \quad (24)$$

The contribution of the planet to the circular velocity is always positive. As was pointed out in Sec. 3.1, circular orbits were not possible near the ring's centre due to a lack of mass in this region of space. But if the planet has enough mass, the square of the circular velocity can be made non-negative everywhere. This happens if  $m/(\sigma_c a^2) \geq 4\pi\sqrt{5}/375 \approx 0.075$ . In Fig. 8 we display some rotation curves, where  $\bar{v}_c = v_c/\sqrt{\sigma_c G a}$  is the dimensionless velocity and where we defined  $\alpha = m/(\sigma_c a^2)$ . By equation (24), the contribution of the central mass to the epicyclic frequency is positive, so it helps to stabilize the circular orbits in the plane of the ring. In fact, it can be shown that if

$$\frac{m}{\sigma_c a^2} \geq \frac{\pi}{3675} (65\sqrt{19} - 41\sqrt{35}) \sqrt{70 - 2\sqrt{665}} \approx 0.15, \quad (25)$$

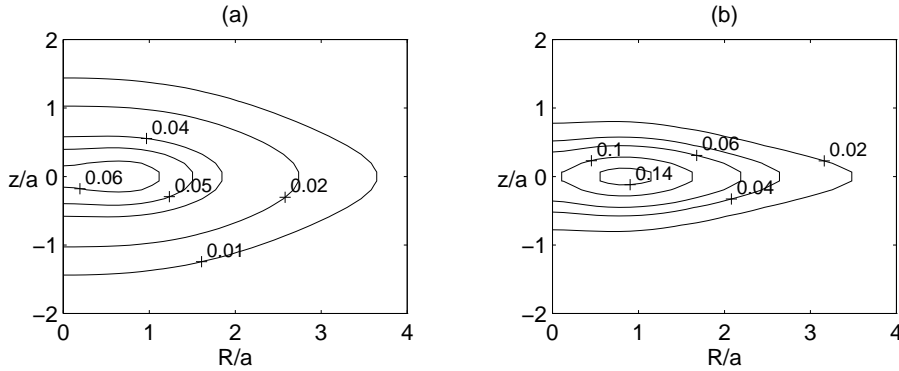


Figure 9: Isodensity curves of the mass density  $\rho^{(1,0)}/(\sigma_c/a)$  equation (27) for a thick single ring as functions of  $R/a$  and  $z/a$ . Parameters: (a)  $b/a = 1$  and (b)  $b/a = 0.5$ .

the epicyclic frequency is always non-negative.

## 4 Thick Rings

Until now all ring structures presented were flat, i.e., had infinitesimal thickness. One way to generate three-dimensional potential-density pairs from these flat ring models is to employ the same transformation used by Miyamoto and Nagai [17] to “inflate” the Kuzmin-Toomre discs.

As a first example, we take the potential  $\phi^{(1,0)}$  of the first member of the family of single rings and apply a transformation  $|z| \rightarrow \sqrt{z^2 + b^2}$ , where  $b$  is a non-negative constant, to equation (34). The resulting mass density is calculated directly from the Poisson equation in cylindrical coordinates

$$\rho = \frac{1}{4\pi G} \left( \phi_{,RR} + \frac{\phi_{,R}}{R} + \phi_{,zz} \right). \quad (26)$$

We obtain

$$\rho^{(1,0)} = \frac{\sigma_c a^2 b^2}{2\xi^3 [R^2 + (a + \xi)^2]^{7/2}} \left\{ aR^4 + R^2(a + \xi) [a^2 + 2\xi(3a + \xi)] + 2\xi^2(a + \xi)^3 \right\}, \quad (27)$$

where  $\xi = \sqrt{z^2 + b^2}$ .

By inspection, the mass density equation (27) is non-negative and free of singularities. Fig. 9(a)–(b) show some isodensity curves of  $\rho^{(1,0)}/(\sigma_c/a)$  as functions of  $R/a$  and  $z/a$  with parameters  $b/a = 1$  in Fig. 9(a) and  $b/a = 0.5$

in Fig. 9(b). For this last parameter value, it is seen that we have a toroidal mass distribution. We also “inflated” the single ring with potential  $\phi^{(1,1)}$  and found a three-dimensional mass density with similar properties.

It is also interesting to compute the rotation curve and epicyclic frequency of particles orbiting the symmetry plane  $z = 0$  of the “inflated” ring. We get

$$v_{c(\text{th.})}^{(1,0)} = R \left\{ \frac{2\pi\sigma_c G a^2 [2R^2 - (a+b)(a-2b)]}{3 [R^2 + (a+b)^2]^{5/2}} \right\}^{1/2}, \quad (28)$$

$$\kappa_{\text{th.}}^{(1,0)} = \left\{ \frac{2\pi\sigma_c G a^2}{3 [R^2 + (a+b)^2]^{7/2}} [2R^4 + R^2(a+b)(13a+10b) - 4(a+b)^3(a-2b)] \right\}^{1/2}, \quad (29)$$

where the subscript th. refers to thick structures. As the thickening parameter  $b/a$  is increased, the regions with impossible and unstable circular orbits shrink until they disappear when  $b/a \geq 1/2$ . On the other hand, Fig. 9 suggest that prominent toroidal mass distributions are formed for  $b/a \leq 1/2$ , and these still have regions with impossible and unstable circular orbits.

If we apply a Miyamoto-Nagai transformation to the potential of two concentric flat rings, we expect to generate two toroidal mass distributions. For instance, the potential  $\phi_{(2)}^{(1,2)}$  equation (19) yields a somewhat involved expression for the density,

$$\begin{aligned} \rho_{(2)}^{(1,2)} = & \frac{\sigma_c a^2 b^2}{70\xi^3 [R^2 + (a+\xi)^2]^{11/2}} \left\{ 35ak^4 R^8 + R^6 [2\xi^3(3-8k^2+24k^4) \right. \\ & + 35ak^4 \xi(11a+10\xi) + 35k^2 a^3(k^2-2)] + R^4(a+\xi)[6\xi^4(3-8k^2+24k^4) \\ & + a\xi^3(48-128k^2+699k^4) + 5a^2\xi^2(7-112k^2+126k^4) - 35a^3\xi(1+20k^2) + 35a^4(1-2k^2)] \\ & + R^2(a+\xi)^3 [6\xi^4(3-8k^2+24k^4) + 2a\xi^3(39-104k^2+172k^4) + 5a^2\xi^2(21-112k^2) \\ & \left. + 5a^3(7a+56\xi)] + 2\xi^2(a+\xi)^5 [\xi^2(3-8k^2+24k^4) + 2a\xi(9-24k^2+2k^4) + 35a^2] \right\}, \end{aligned} \quad (30)$$

where  $\xi = \sqrt{z^2 + b^2}$ .

Some isodensity curves of the mass density  $\rho_{(2)}^{(1,2)}/(\sigma_c/a)$  are displayed in Fig. 10(a)–(b) with parameters  $k = 1$ ,  $b/a = 0.5$  in Fig. 10(a) and  $k = 1$ ,

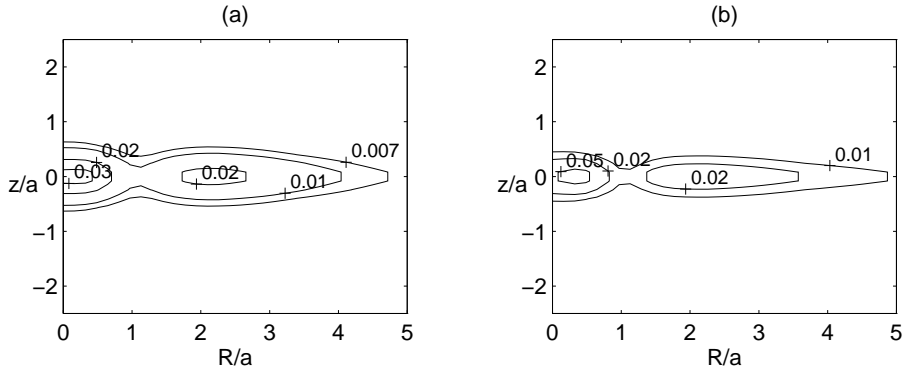


Figure 10: Isodensity curves of the mass density  $\rho_{(2)}^{(1,2)}/(\sigma_c/a)$  equation (30) for a thick double ring as functions of  $R/a$  and  $z/a$ . Parameters (a)  $k = 1$ ,  $b/a = 0.5$  and (b)  $k = 1$ ,  $b/a = 0.3$ .

$b/a = 0.3$  in Fig. 10(b). For this set of parameters, the mass density is positive everywhere. We also tested it for some other values of  $k$  and  $b/a$  and did not find regions with negative mass density or singularities.

For this two-toroid system, we also computed the rotation curve and epicyclic frequency. The explicit expressions are given in Appendix F. Fig. 11(a) shows some zero velocity curves of equation (50) and Fig. 11(b) curves of zero epicyclic frequency equation (51) as functions of  $R/a$  and  $k$  for the thickening parameters  $b/a = 0$ ,  $b/a = 0.25$  and  $b/a = 0.5$ . Here, thickening also helps to stabilize circular orbits and shrinks the regions with negative square velocities.

## 5 Discussion

We presented some families of analytical potential-density pairs that represent one or two concentric flat rings that were constructed by superposing members of the Kuzmin-Toomre family of discs, and also a disc surrounded by a flat ring. All potential-density pairs can be expressed in terms of elementary functions. Although the models have infinite extension, the surface density decays with the distance very fast, and, in principle, one can insert a clear cut-off and consider them as finite. For these models, we studied the circular orbits of test particles concentric to the rings and made a first study of the stability of these structures by radial perturbations of circular orbits (epicyclic frequency). In general the two-ring structures tend to be



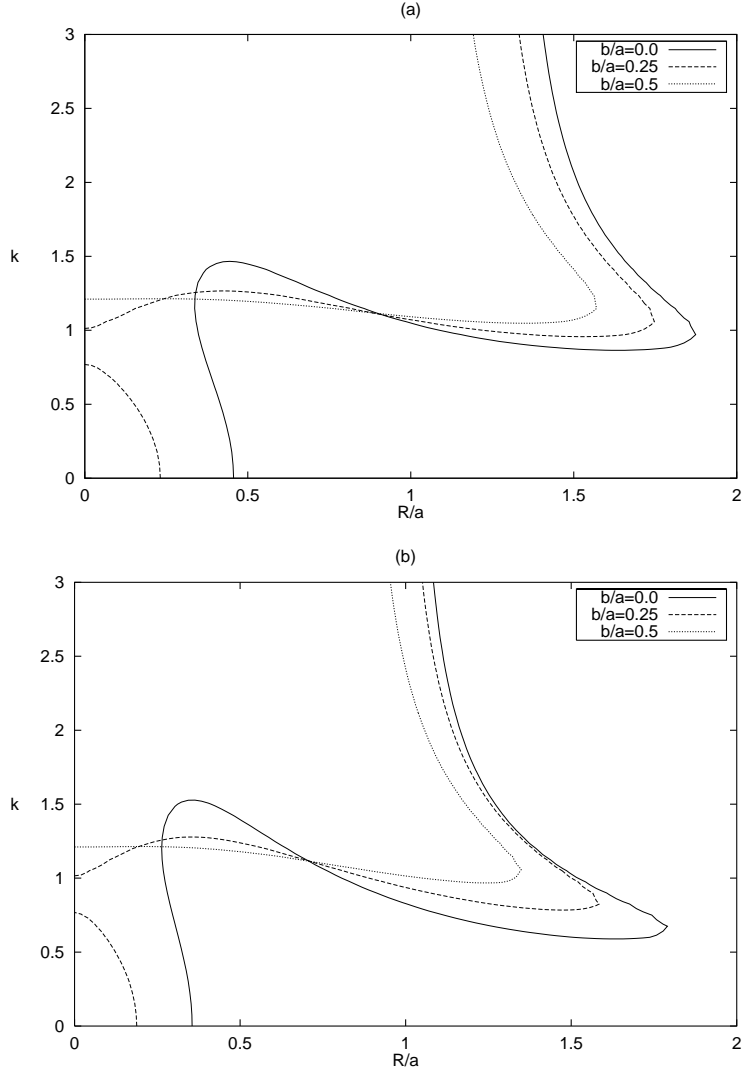


Figure 11: (a) Curves of  $v_{c(2)\text{th.}}^{(1,2)} = 0$  equation (50) and (b)  $\kappa_{c(2)\text{th.}}^{(1,2)} = 0$  equation (51) for a thick double ring as functions of  $R/a$  and  $k$  for  $b/a = 0$ ,  $b/a = 0.25$  and  $b/a = 0.5$ .

more unstable than the single rings, and a surrounding ring also helps to destabilize a disc. On the other hand, if we put a planet located at the centre of a ring it tends to increase stability in the radial direction.

We also presented two examples of “inflated” rings that were obtained by applying a Miyamoto-Nagai like transformation on the above-mentioned single and double flat rings. The resulting three-dimensional mass densities have a toroidal shape, are non-negative and free of singularities. The thickening of flat ring structures increases stability in the radial direction.

As was mentioned, a first stability test of the presented ring structures was based on the study of stability of individual particles. The study of stability of orbits perpendicular to the plane of flat rings is not trivial because of the abrupt change of matter density as a particle crosses the plane of the ring. For instance, Saa and Venegeroles [23] showed that the presence of a thin plane destroys the integrability of orbits of particles that cross the plane and these orbits tend to be chaotic. This effect is similar to the behaviour of the Chua circuit, a well-known case of chaotic system [24]. Recently, [25] studied the stability of orbits crossing Morgan and Morgan discs, thin finite discs.

A more realistic approach should take into account collective effects. The stability of the gravitating system will be determined by the behaviour of the perturbation of the matter content of the disk. Some examples of a General Relativistic stability analysis of discs can be found in [26, 27].

## Acknowledgments

We thank FAPESP for financial support, PSL also thanks CNPq. This research has made use of SAO/NASA’s Astrophysics Data System abstract service, which is gratefully acknowledged.

## References

- [1] Fridman A.M., Gorkavyi N.N., 1999, *Physics of Planetary Rings*. Springer-Verlag, Heidelberg
- [2] Theys J.C., Spiegel E.A., 1976, *ApJ*, 208, 650
- [3] Theys J.C., Spiegel E.A., 1977, *ApJ*, 212, 616
- [4] Whitmore B.C., Lucas R.A., McElroy D.B., Steiman-Cameron T.Y., Sackett P.D., Olling R.P., 1990, *AJ*, 100, 1489

- [5] Appell P., 1887, *Ann. Math., Lpz.*, 30, 155
- [6] Whittaker E.T., Watson G.N., 1950, *A Course of Modern Analysis*, 4th edn. Cambridge Univ. Press, Cambridge
- [7] Gleiser R., Pullin J., 1989, *Class. Quantum Grav.*, 6, 977
- [8] Letelier P.S., Oliveira S.R., 1998, *Class. Quantum Grav.*, 15, 421
- [9] Lemos J.P.S., Letelier P.S., 1994, *Phys. Rev. D*, 49, 5135
- [10] Chakrabarti S.K., 1988, *JA&A.*, 9, 49
- [11] Semerák O., Žáček M., Zellerin T., 1999, *MNRAS*, 308, 705
- [12] Semerák O., Zellerin T., Žáček M., 1999, *MNRAS*, 308, 691
- [13] Letelier P.S., 2007, *MNRAS*, 381, 1031
- [14] Morgan T., Morgan L., 1969, *Phys. Rev.*, 183, 1097
- [15] Ciotti L., Giampieri G., 2007, *MNRAS*, 376, 1162
- [16] Ciotti L., Marinacci F., 2008, *MNRAS*, 387, 1117
- [17] Miyamoto M., Nagai R., 1975, *PASJ*, 27, 533
- [18] Kuzmin G.G., 1956, *AZh.*, 33, 27
- [19] Toomre A., 1963, *ApJ*, 138, 385
- [20] Nagai R., Miyamoto M., 1976, *PASJ*, 28, 1
- [21] Bičák J., Lynden-Bell D., Pichon C., 1993, *MNRAS*, 265, 126
- [22] Binney J., Tremaine S., 2008, *Galactic Dynamics*, 2nd edn. Princeton Univ. Press, Princeton, NJ
- [23] Saa A., Venegeroles R., 1999, *Phys. Lett. A*, 259, 201
- [24] Chua L., Komuro M., Matsumoto T., 1986, *IEEE Transactions on Circuit and Systems*, 33, 1072
- [25] Caro J.R., Suspes F.L., González G.A., 2008, *MNRAS*, 386, 440
- [26] Ujevic M., Letelier P.S., 2004, *Phys. Rev. D*, 70, 084015
- [27] Ujevic M., Letelier P.S., 2007, *Gen. Rel. Grav.*, 39, 1345

## A Potential-density pairs for Kuzmin-Toomre discs

The explicit expressions for the density and potentials for Kuzmin-Toomre discs with with  $n = 1, 2, 3$  are

$$\sigma_1 = \frac{3a^3 M}{2\pi(R^2 + a^2)^{5/2}}, \quad \phi_1 = -\frac{GM}{[R^2 + (a + |z|)^2]^{3/2}} (R^2 + |z|^2 + 2a^2 + 3a|z|), \quad (31)$$

$$\sigma_2 = \frac{5a^5 M}{2\pi(R^2 + a^2)^{7/2}}, \quad \phi_2 = -\frac{GM}{3[R^2 + (a + |z|)^2]^{5/2}} \left\{ 3[R^2 + (a + |z|)^2] \right. \\ \left. \times [R^2 + (a + |z|)^2 + a(a + |z|)] - a^2[R^2 - 2(a + |z|)^2] \right\}, \quad (32)$$

$$\sigma_3 = \frac{7a^7 M}{2\pi(R^2 + a^2)^{9/2}}, \quad \phi_3 = -\frac{GM}{5[R^2 + (a + |z|)^2]^{7/2}} \left\{ 5[R^2 + (a + |z|)^2]^3 \right. \\ \left. + a[R^2 + (a + |z|)^2]^2(4a + 5|z|) + a^2[R^2 + (a + |z|)^2] [-R^2 + 5|z|(a + |z|)] \right. \\ \left. + a^3(a + |z|)[2R^2 + 7(a + |z|)^2] \right\}. \quad (33)$$

## B Potential-density pairs for flat one rings

The explicit expressions for the density and potentials of four members of flat one rings with  $m = 1, 2$ ;  $n = 0, 1$  read

$$\sigma^{(1,0)} = \frac{\sigma_c (R/a)^2}{(1 + R^2/a^2)^{5/2}}, \quad \phi^{(1,0)} = -\frac{2\pi\sigma_c G a^2}{3[R^2 + (a + |z|)^2]^{3/2}} (2R^2 + 2|z|^2 + a^2 + 3a|z|), \quad (34)$$

$$\sigma^{(1,1)} = \frac{\sigma_c (R/a)^2}{(1 + R^2/a^2)^{7/2}}, \quad \phi^{(1,1)} = -\frac{2\pi\sigma_c G a^2}{15[R^2 + (a + |z|)^2]^{5/2}} \left[ R^2(2R^2 + 2|z|^2 + 5a^2 + 6a|z|) + 2(a + |z|)^2(R^2 + |z|^2 + a^2 + 3a|z|) \right], \quad (35)$$

$$\sigma^{(2,0)} = \frac{\sigma_c (R/a)^4}{(1 + R^2/a^2)^{7/2}}, \quad \phi^{(2,0)} = -\frac{2\pi\sigma_c G a^2}{15[R^2 + (a + |z|)^2]^{5/2}} \left\{ [R^2 + (a + |z|)^2] \times (8R^2 + 8|z|^2 + 9a|z|) + 3a^2(a + |z|)^2 \right\}, \quad (36)$$

$$\sigma^{(2,1)} = \frac{\sigma_c (R/a)^4}{(1 + R^2/a^2)^{9/2}}, \quad \phi^{(2,1)} = -\frac{2\pi\sigma_c G a^2}{105[R^2 + (a + |z|)^2]^{7/2}} \left\{ [R^2 + (a + |z|)^2]^2 \times (8R^2 + 8|z|^2 + 13a^2 + 24a|z|) + a^2[R^2 + (a + |z|)^2] \times (11R^2 - 13|z|^2 - 28a^2 - 41a|z|) + 3a^3(a + |z|)[2R^2 + 7(a + |z|)^2] \right\}. \quad (37)$$

## C Rotation curves and epicyclic frequency for flat one rings

The expressions for the circular velocity  $v_c^{(m,n)}$  and the regions with non-negative velocity for the members of flat one rings (34)–(37) are given by

$$v_c^{(1,0)} = R \left[ \frac{2\pi\sigma_c G a^2 (2R^2 - a^2)}{3(R^2 + a^2)^{5/2}} \right]^{1/2}, \quad v_c^{(1,0)} \geq 0 \text{ for } \frac{R}{a} \geq \frac{\sqrt{2}}{2} \approx 0.71, \quad (38)$$

$$v_c^{(1,1)} = R \left[ \frac{2\pi\sigma_c G a^2}{15(R^2 + a^2)^{7/2}} (2R^4 + 13R^2 a^2 - 4a^4) \right]^{1/2},$$

$$v_c^{(1,1)} \geq 0 \text{ for } \frac{R}{a} \geq \frac{\sqrt{\sqrt{201} - 13}}{2} \approx 0.54, \quad (39)$$

$$v_c^{(2,0)} = R \left[ \frac{2\pi\sigma_c G a^2}{15(R^2 + a^2)^{7/2}} (8R^4 - 8R^2 a^2 - a^4) \right]^{1/2},$$

$$v_c^{(2,0)} \geq 0 \text{ for } \frac{R}{a} \geq \frac{\sqrt{\sqrt{6} + 2}}{2} \approx 1.05, \quad (40)$$

$$v_c^{(2,1)} = R \left[ \frac{2\pi\sigma_c G a^2}{105(R^2 + a^2)^{9/2}} (8R^6 + 72R^4 a^2 - 45R^2 a^4 - 4a^6) \right]^{1/2},$$

$$v_c^{(2,1)} \geq 0 \text{ for } \frac{R}{a} \gtrsim 0.81. \quad (41)$$

The corresponding expressions for the epicyclic frequency  $\kappa^{(m,n)}$  and the regions of stability read

$$\kappa^{(1,0)} = \left[ \frac{2\pi\sigma_c G a^2}{3(R^2 + a^2)^{7/2}} (2R^4 + 13R^2 a^2 - 4a^4) \right]^{1/2},$$

$$\text{stable for } \frac{R}{a} \geq \frac{\sqrt{\sqrt{201} - 13}}{2} \approx 0.54, \quad (42)$$

$$\kappa^{(1,1)} = \left[ \frac{2\pi\sigma_c G a^2}{15(R^2 + a^2)^{9/2}} (2R^6 + 3R^4 a^2 + 90R^2 a^4 - 16a^6) \right]^{1/2},$$

$$\text{stable for } \frac{R}{a} \gtrsim 0.42, \quad (43)$$

$$\kappa^{(2,0)} = \left[ \frac{2\pi\sigma_c G a^2}{15(R^2 + a^2)^{9/2}} (8R^6 + 72R^4 a^2 - 45R^2 a^4 - 4a^6) \right]^{1/2},$$

$$\text{stable for } \frac{R}{a} \gtrsim 0.81, \quad (44)$$

$$\kappa^{(2,1)} = \left[ \frac{2\pi\sigma_c G a^2}{105(R^2 + a^2)^{11/2}} (8R^8 + 8R^6 a^2 + 711R^4 a^4 - 250R^2 a^6 - 16a^8) \right]^{1/2},$$

$$\text{stable for } \frac{R}{a} \gtrsim 0.64. \quad (45)$$

## D Rotation curves and epicyclic frequency for flat two rings

The expressions for the circular velocity  $v_{c(2)}^{(1,2)}$  and the epicyclic frequency  $\kappa_{(2)}^{(1,2)}$  for a particular member of two flat rings studied in Section 3.2 are given by

$$v_{c(2)}^{(1,2)} = R \left\{ \frac{2\pi\sigma_c G a^2}{105(R^2 + a^2)^{9/2}} [2R^6(3 - 8k^2 + 24k^4) - 3R^4 a^2(-11 + 48k^2 + 24k^4) + 18R^2 a^4(6 + 5k^2 - k^4) - a^6(24 - 8k^2 + 3k^4)] \right\}^{1/2}, \quad (46)$$

$$\kappa_{(2)}^{(1,2)} = \left\{ \frac{2\pi\sigma_c G a^2}{105(R^2 + a^2)^{11/2}} [2R^8(3 - 8k^2 + 24k^4) + R^6 a^2(27 - 16k^2 + 552k^4) - 6R^4 a^4(10 + 237k^2 + 87k^4) + R^2 a^6(768 + 500k^2 - 93k^4) - 4a^8(24 - 8k^2 + 3k^4)] \right\}^{1/2}. \quad (47)$$

## E Rotation curves and epicyclic frequency for discs with flat rings

The expressions for the circular velocity  $v_{c(d)}^{(2)}$  and the epicyclic frequency  $\kappa_{(d)}^{(2)}$  for a particular member of the disc with a flat ring studied in Section 3.3 are given by

$$v_{c(d)}^{(2)} = R \left\{ \frac{2\pi\sigma_c G a^2}{15(R^2 + a^2)^{7/2}} [R^4(3 - 4k^2 + 8k^4) - 2R^2 a^2(-6 + 13k^2 + 4k^4) + a^4(24 + 8k^2 - k^4)] \right\}^{1/2}, \quad (48)$$

$$\kappa_{(d)}^{(2)} = \left\{ \frac{2\pi\sigma_c G a^2}{15(R^2 + a^2)^{9/2}} [R^6(3 - 4k^2 + 8k^4) + 6R^4 a^2(2 - k^2 + 12k^4) - 45R^2 a^4 k^2(4 + k^2) + 4a^6(24 + 8k^2 - k^4)] \right\}^{1/2}. \quad (49)$$

## F Rotation curves and epicyclic frequency for thick two rings

The expressions for the circular velocity  $v_{c(2)\text{th.}}^{(1,2)}$  and the epicyclic frequency  $\kappa_{(2)\text{th.}}^{(1,2)}$  for a particular member of thick two rings studied in Section 4 are



given by

$$\begin{aligned}
v_{c(2)\text{th.}}^{(1,2)} &= R \left\{ \frac{2\pi\sigma_c G a^2}{105 [R^2 + (a+b)^2]^{9/2}} \{ 2R^6(3 - 8k^2 + 24k^4) \right. \\
&+ 3R^4 [-a^2(-11 + 48k^2 + 24k^4) + 3ab(6 - 16k^2 + 13k^4) + 2b^2(3 - 8k^2 + 24k^4)] \\
&+ 3R^2(a+b)[6a^3(6 + 5k^2 - k^4) + 2b^3(3 - 8k^2 + 24k^4) + 10ab^2(3 - 8k^2 + 3k^4) \\
&- a^2b(-45 + 64k^2 + 39k^4)] - (a+b)^3 [a^3(24 - 8k^2 + 3k^4) - 2b^3(3 - 8k^2 + 24k^4) \\
&\left. + 3ab^2(-12 + 32k^2 + 9k^4) - 6a^2b(11 + 8k^2 - 3k^4)] \} \}^{1/2}, \quad (50) \\
\kappa_{(2)\text{th.}}^{(1,2)} &= \left\{ \frac{2\pi\sigma_c G a^2}{105 [R^2 + (a+b)^2]^{11/2}} \{ 2R^8(3 - 8k^2 + 24k^4) \right. \\
&+ R^6 [a^2(27 - 16k^2 + 552k^4) + ab(66 - 176k^2 + 843k^4) + 14b^2(3 - 8k^2 + 24k^4)] \\
&+ 3R^4(a+b) [-2a^3(10 + 237k^2 + 87k^4) + a^2b(97 - 576k^2 + 237k^4) \\
&+ 2ab^2(51 - 136k^2 + 303k^4) + 10b^3(3 - 8k^2 + 24k^4)] + R^2(a+b)^3 \\
&\quad \times [a^3(768 + 500k^2 - 93k^4) - 12a^2b(-40 + 116k^2 + 51k^4) \\
&\quad + 15ab^2(24 - 64k^2 + 45k^4) + 26b^3(3 - 8k^2 + 24k^4)] - 4(a+b)^5 \\
&\left. \times [a^3(24 - 8k^2 + 3k^4) + 6a^2b(-11 - 8k^2 + 3k^4) + 3ab^2(-12 + 32k^2 + 9k^4) \right. \\
&\quad \left. - 2b^3(3 - 8k^2 + 24k^4)] \} \}^{1/2}. \quad (51)
\end{aligned}$$